

9.3

HIGH-RESOLUTION MODELING OF THE 25 DECEMBER 2002 NORTHEAST U.S. BANDED SNOWSTORM

David R. Novak^{1/2*}, Brian A. Colle¹, and Daniel Keyser³

¹NOAA/NWS Eastern Region Headquarters, Scientific Services Division, Bohemia, New York

²Stony Brook University, State University of New York, Stony Brook, New York

³University at Albany, State University of New York, Albany, New York

1. INTRODUCTION

Mesoscale band formation on the poleward side of extratropical cyclones can dramatically affect precipitation intensity and amount. These bands are favored during the cold season, and are often associated with midlevel frontogenesis in the presence of weak moist symmetric stability and sufficient moisture (Thorpe and Emanuel 1985; Nicosia and Grumm 1999; Novak et al. 2004a). Several observational case studies have focused on the development and evolution of such bands (e.g., Sanders and Bosart 1985). However, studies investigating high-resolution (≤ 12 km) modeling of these features have been limited (e.g., Han et al. 2003). Given the impact cold season mesoscale band formation has on precipitation intensity and amount, there is a need to further explore the capability of high-resolution models to simulate such cold season mesoscale banding events.

This study will use the fifth-generation Penn State/NCAR Mesoscale Model (MM5) and Weather Research and Forecasting (WRF) modeling frameworks to explore the capabilities of high-resolution models to simulate the development of banded precipitation during the 25 December 2002 snowstorm. Particular emphasis is placed on comparing the MM5 and WRF forecasts of the mesoscale band observed during this case.

2. CASE STUDY DESIGN

For purposes of this study an observed band is defined as the occurrence of a linear reflectivity structure > 250 km in length, 20–100 km in width, with an intensity > 30 dBZ maintained for at least 2 h. This definition corresponds to the single band type in the band classification scheme proposed by Novak et al. (2004a). Based on the above length and width criteria, the surface simulated reflectivity field from the MM5 and WRF were subjectively evaluated to determine if the models forecast banding. The intensity criterion was not strictly considered when evaluating the model forecasts given uncertainties in the calibration of simulated reflectivity algorithms (Stoelinga 2005).

To facilitate model comparisons, MM5 (v3.4.0) and WRF (v2.0.3) were run retrospectively with identical initial conditions [0000 UTC 25 December 2002 Eta Data Assimilation System (EDAS) analysis on a 32 km grid] and physics (to the extent possible). For this case it was subjectively determined that the use of the Grell convective parameterization (Grell 1993), the National Centers for Environmental Prediction (NCEP) Medium-Range Forecast (MRF) boundary layer scheme (Hong and Pan 1996), and

simple ice microphysics (Dudhia 1989; Hong et al. 2004) gave simulations most similar to the observed evolution of the cyclone and associated mesoscale band. Both the MM5 and WRF simulations were integrated for an outer 36-km domain, and 12-km and 4-km (one way) nested domains centered on the simulated banding location over eastern New York. The 4 km nest was run using explicit convection. Comparisons of the MM5 and WRF model forecasts with the 0000 UTC 25 December 2002 operational run of the NCEP Eta model (renamed the North American Mesoscale model in January 2005) are also made for select fields.

To explore the predictability of the 25 December 2002 case, an ensemble of simulations using different initial conditions, convective parameterizations, and boundary layer and microphysics schemes were run using the MM5 and WRF modeling frameworks. All members in the ensemble system were initialized at 0000 UTC 25 December 2002.

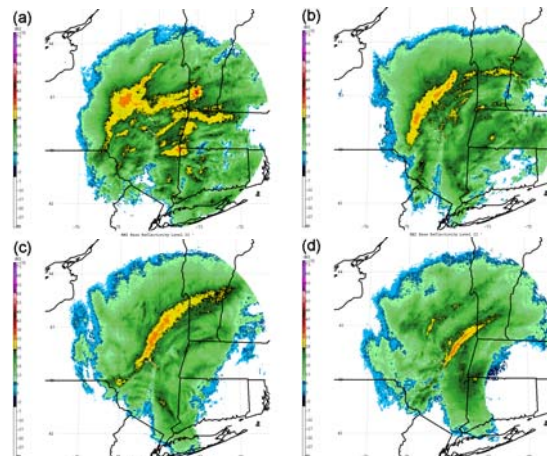


Fig. 1. Albany, New York (ENX), WSR-88D radar reflectivity (shaded according to scale, dBZ) at (a) 2002 UTC, (b) 2200 UTC, and (c) 2358 UTC 25 Dec 2002, and (d) 0158 UTC 26 Dec 2002.

3. CASE OVERVIEW

The 25 December 2002 snowstorm was a historic event for central and eastern New York, with storm total snowfall accumulations exceeding 91 cm (36 in.) in some locations. Much of this snow fell during a 12-h period associated with an intense mesoscale snowband (Fig. 1). The snowband developed in central New York shortly after 1900 UTC 25 December 2002 (Fig. 1a), reached maturity near 2200 UTC (Fig. 1b), and slowly shifted east into eastern New York and weakened by 0200 UTC 26 December 2002 (Figs. 1c,d).

*Corresponding author address: David Novak, NOAA/NWS Eastern Region Headquarters, 630 Johnson Avenue, Suite 202, Bohemia, NY 11716. Email: david.novak@noaa.gov

Snowfall rates of 13 cm h^{-1} (5 in. h^{-1}) were officially recorded as the band moved through Albany, New York, around 0100 UTC 26 December 2002.

Rapid Update Cycle (RUC) analyses (not shown, see Novak et al. 2004b) show that the snowband developed northwest of the deepening surface cyclone as the midlevel (700 hPa) low formed. Strong frontogenesis and weak moist symmetric stability developed within the deformation zone just north of the deepening midlevel low by 1800 UTC 25 December 2002, and were correlated with the general location of the initial band formation over central New York. The frontogenesis maximum, moist symmetric stability minimum, and associated heavy precipitation slowly shifted east as the cyclone continued to deepen. This evolution is consistent with climatological studies of banded cyclones in the northeast United States (e.g., Nicosia and Grumm 1999; Novak et al. 2004a).

4. RESULTS

4.1 MM5 and WRF comparison

The MM5 and WRF accurately predicted cyclogenesis, with forecast surface cyclone tracks within 50 km of the observed track. However, only the WRF was able to adequately forecast the rapid cyclone intensification, with the MM5 as well as the operational Eta significantly underpredicting the cyclone depth (Fig. 2). Storm total accumulated precipitation further illustrates the challenge this case presented to models. The observed accumulated precipitation (liquid equivalent) during the 24-h period ending

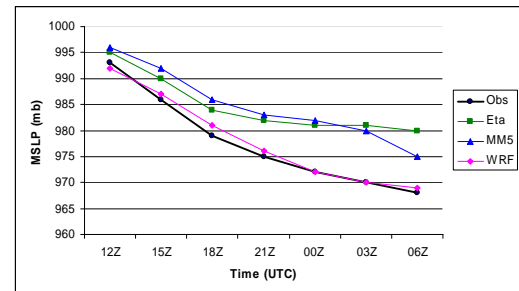


Fig. 2. Time series of the observed and forecast surface cyclone central pressure from 1200 UTC 25 Dec 2002 to 0600 UTC 26 Dec 2002.

1200 UTC 26 December is shown in Fig. 3a. A band of greater than 2.00 in. (50.8 mm) was observed extending from northeastern Pennsylvania into eastern New York, corresponding to the mesoscale band location. A maximum storm total liquid equivalent of 3.00 in. (76.2 mm) was observed within this band over eastern New York. Comparisons of the observed precipitation to the operational 12 km Eta, MM5, and WRF model forecasts showed that although the Eta and MM5 models depicted the precipitation maximum in eastern New York, the precipitation maximum was underforecast by $\sim 50\%$ and $\sim 40\%$, respectively. In contrast, the WRF model forecast precipitation amounts are comparable to the observed amounts; however, the forecast precipitation maximum was located in eastern Pennsylvania, which was well to the south of the observed maximum.

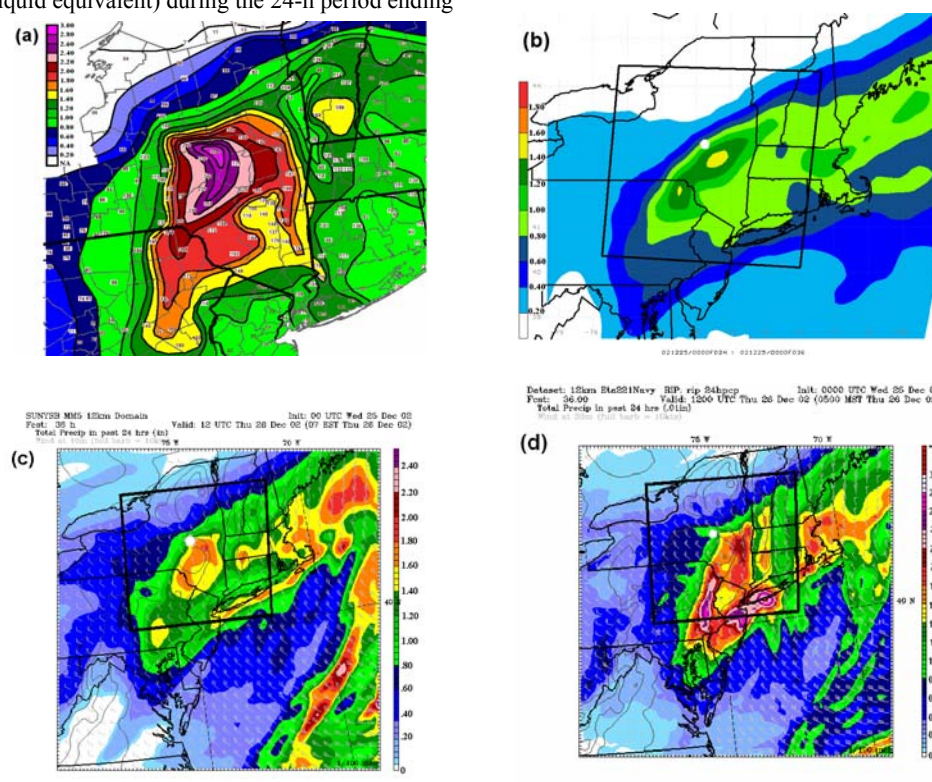


Fig. 3. (a) Observed storm total precipitation (shaded according to color scale every 0.20 in.). (b) Forecast accumulated precipitation during the 24-h period ending 1200 UTC 26 December 2002 from the 12 km Eta, (c) MM5, and (d) WRF. The domain of Fig. 3a and the location of observed maximum precipitation (white dot) is shown for reference on Figs. 3b–d.

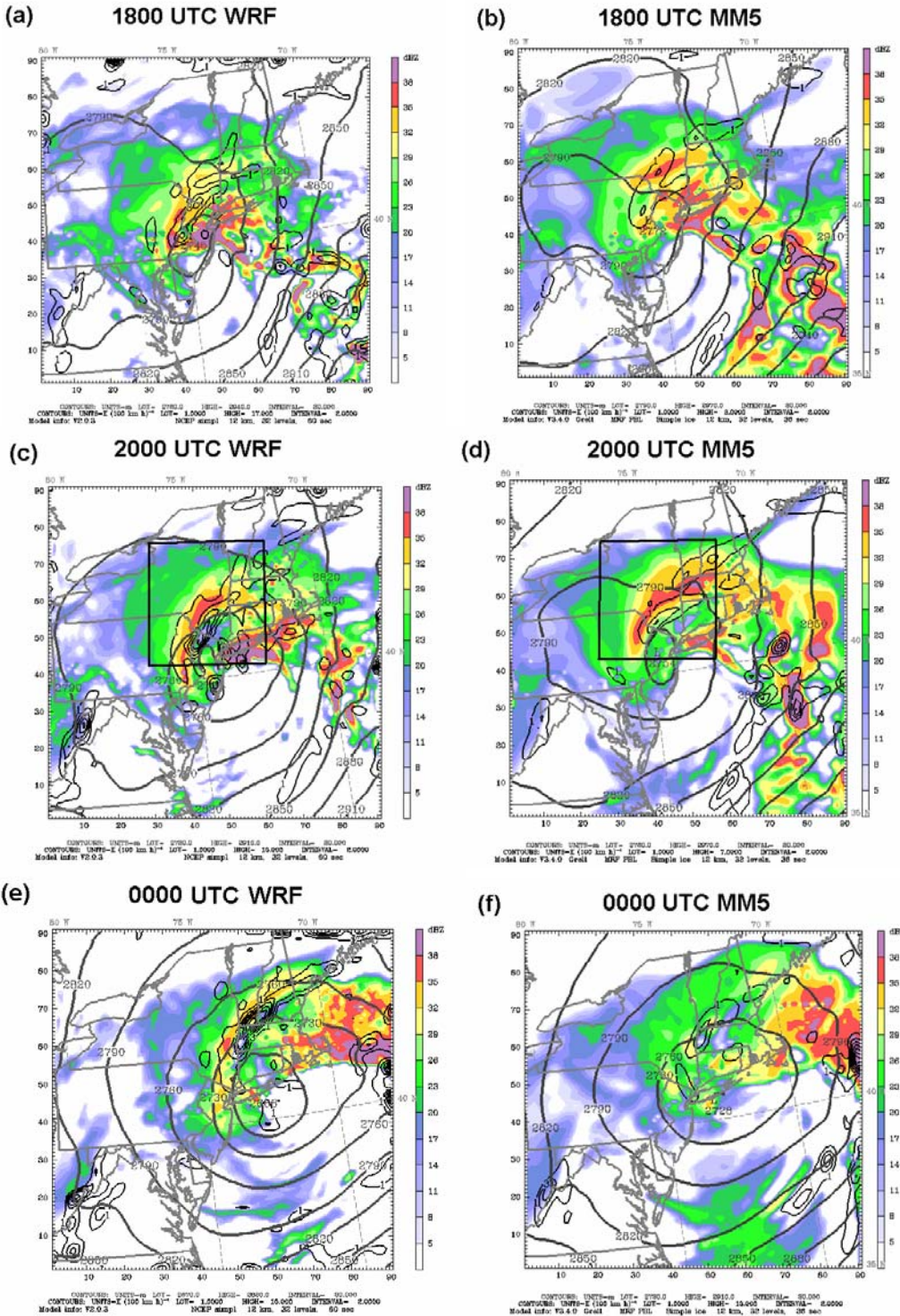


Fig. 4. (a) 12-km WRF 18-h forecast surface simulated reflectivity (shaded according to scale starting at 5 dBZ), 700-hPa geopotential height (thick gray, contoured every 3 dam), and 700-hPa Miller 2D frontogenesis [thin solid, positive values contoured every $2^{\circ}\text{C} (100 \text{ km})^{-1} \text{ h}^{-1}$ starting at $1^{\circ}\text{C} (100 \text{ km})^{-1} \text{ h}^{-1}$] valid at 1800 UTC 25 Dec 2002. (b) Same as in (a), except for 12-km MM5. (c) Same as in (a), except for 12-km WRF 20-h forecast valid at 2000 UTC 25 Dec 2002. (d) Same as in (a), except for 12-km MM5 20-h forecast valid at 2000 UTC 25 Dec 2002. (e) Same as in (a), except for 12-km WRF 24-h forecast valid at 0000 UTC 26 Dec 2002. (f) Same as in (a), except for 12-km MM5 24-h forecast valid at 0000 UTC 26 Dec 2002.

Given the association of band development with midlevel frontogenesis, weak moist symmetric stability, and sufficient moisture, these parameters were assessed in the MM5 and WRF model forecasts. Both model forecasts show that frontogenesis developed within the deformation zone just north of the developing midlevel low by 1800 UTC 25 December 2002 (Figs. 4a,b). However, at this time the WRF 700-hPa low center was 33 m deeper and approximately 50 km farther southeast than the MM5 700-hPa low center. Consequently the midlevel deformation and associated frontogenesis maximum in the WRF simulation was farther southeast than in the MM5. These differences in the location of the midlevel frontogenesis maximum led to differences in the location of initial band development, with the WRF forecasting initial band development over eastern Pennsylvania, while the MM5 forecast band development over eastern New York. It is interesting to note that the observed initial band development over central New York around 1900 UTC is most consistent with the MM5 model forecasts, although the surface cyclone depth was underpredicted by the MM5 model (cf., Fig. 2).

Just two hours later, at 2000 UTC 25 December 2002, intense bands were established in both the MM5 and WRF model forecasts, with respective frontogenesis maxima oriented parallel to the simulated bands (Figs. 4c,d). Over the next four hours the midlevel frontogenesis and associated band in the MM5 model forecast slowly weakened as the band shifted east, such that the band was nearly absent in the forecast fields by 0000 UTC 26 December 2002 (Fig. 4e). The intense band noted in the WRF model at 2000 UTC over northeast Pennsylvania weakened dramatically over the next two hours (not shown), while a second band formed farther east near the New York/Massachusetts border. This second band is evident in the 0000 UTC 26 December 2002 simulated radar reflectivity fields (Fig. 4e), and was associated with a discontinuous eastward shift in the midlevel frontogenesis maximum. The rapid dissipation of the initial band and formation of a second band was not observed, although the location of the second band in the WRF model forecast was near the observed band location at this time (cf. Fig. 1c). The second band dissipated in the WRF model forecast by 0200 UTC 26 December 2002 (not shown).

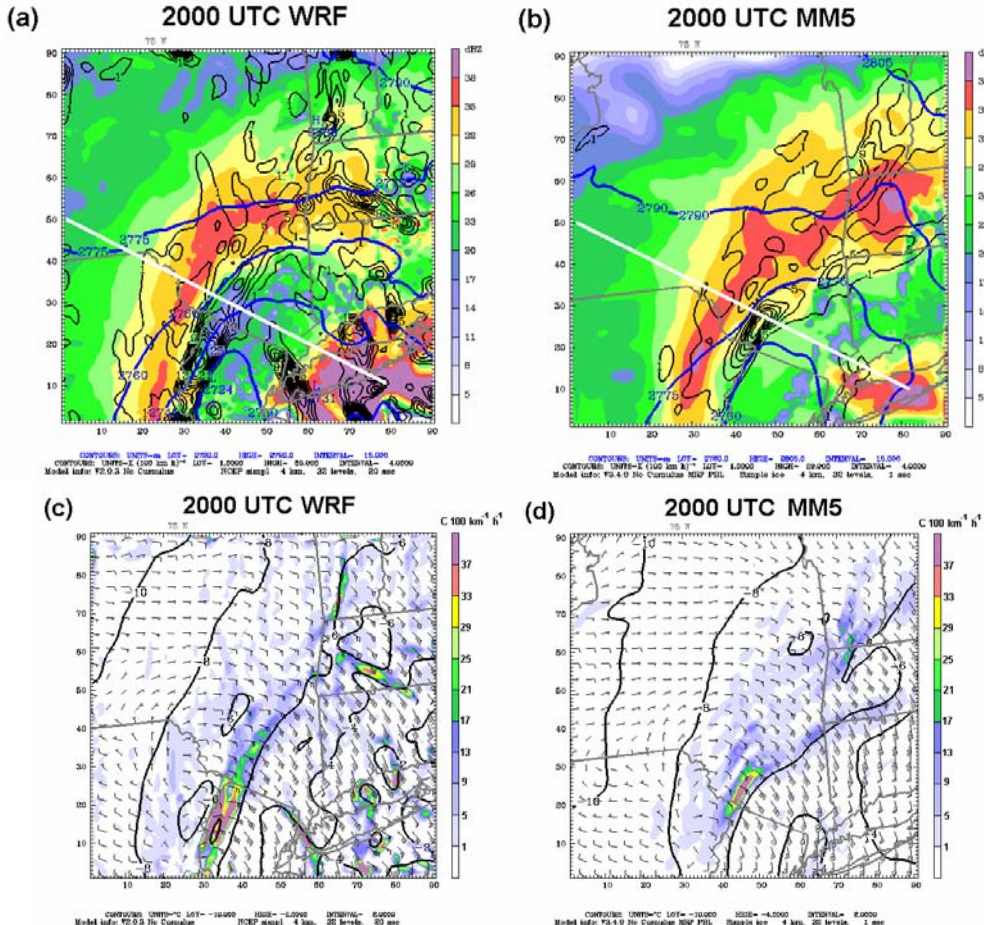


Fig. 5. (a) 4-km WRF (domain shown in Fig. 4c) 20-h forecast surface simulated reflectivity (shaded according to scale starting at 5 dBZ), 700-hPa geopotential height (thick blue, contoured every 15 m), and 700-hPa Miller 2D frontogenesis [thin solid, positive values contoured every 4°C (100 km) $^{-1} \text{ h}^{-1}$] valid at 2000 UTC 25 Dec 2002. (b) Same as in (a), except for the 4-km MM5 forecast (domain shown in Fig. 4d). (c) 4-km WRF 20-h forecast 700-hPa Miller 2D frontogenesis [shaded according to scale starting at 1°C (100 km) $^{-1} \text{ h}^{-1}$], 700-hPa temperature (solid, contoured every 2°C), and 700-hPa wind (1 full barb = 10 kt) valid at 2000 UTC 25 Dec 2002. (d) Same as in (c), except for the 4-km MM5 forecast.

The 4-km nested simulations were similar to the 12-km simulations in terms of the placement of the deformation zone, frontogenesis, and associated band; however, the scale of the frontogenesis and associated band decreased $\sim 30\%$ from that of the 12-km simulation. The 20-h 4-km forecasts (valid at 2000 UTC 25 December 2002) from the WRF (Fig. 5a) and MM5 (Fig. 5b) also show that the magnitude of the forecast 700-hPa frontogenesis maximum increased dramatically compared to the 12-km simulation, with 4-km forecast 700-hPa frontogenesis maxima on the order of 40°C (100 km) $^{-1} \text{ h}^{-1}$ and 30°C (100 km) $^{-1} \text{ h}^{-1}$ for the WRF and MM5 models, respectively. Examination of the wind and temperature fields show that these extreme values of frontogenesis result from a combination speed and directional changes in the wind (consistent with deformation) in the presence of a temperature gradient. For example, southeast winds over 40 kt near the New York/New Jersey state border slow to only 10 kt over a distance of less than 50 km in the vicinity of the respective frontogenesis maxima (Figs. 5c,d). Such speed convergence in the presence of the forecast temperature gradient results in a pronounced gradient in warm air advection. Concurrently, the strong southeast winds on the warm side of the frontogenesis maxima turn sharply and

become north winds on the cold side of the frontogenesis maxima (Figs. 5c,d), changing the sign of the thermal advection in the vicinity of the frontogenesis maximum. Although such extreme wind changes seem possible in the midlevels of developing cyclones, observations on the scale of this feature were not available in this case at this time to verify the model forecast.

Cross sections through the respective forecast bands at 2000 UTC 25 December 2002 show that the precipitation bands extended to nearly 300 hPa, with a narrow, sloping ascent maximum approaching 1 m s^{-1} on the warm side of the frontogenesis maximum (Figs. 6a,b). Weak gravitational stability was noted above the frontogenesis maximum (indicated by the wide separation in saturated equivalent potential temperature contours). To diagnose the symmetric stability, saturation equivalent potential vorticity (EPV^*) was calculated using the full wind. Small areas of negative EPV^* were found in the vicinity of the snowband at the surface and 500 hPa (Figs. 6c,d), although a majority of the ascent region exhibited small positive EPV^* values, suggesting weak moist symmetric stability. The above features noted in the cross sections are consistent with contemporary conceptual models of banded frontal zones (e.g., Moore et al. 2005).

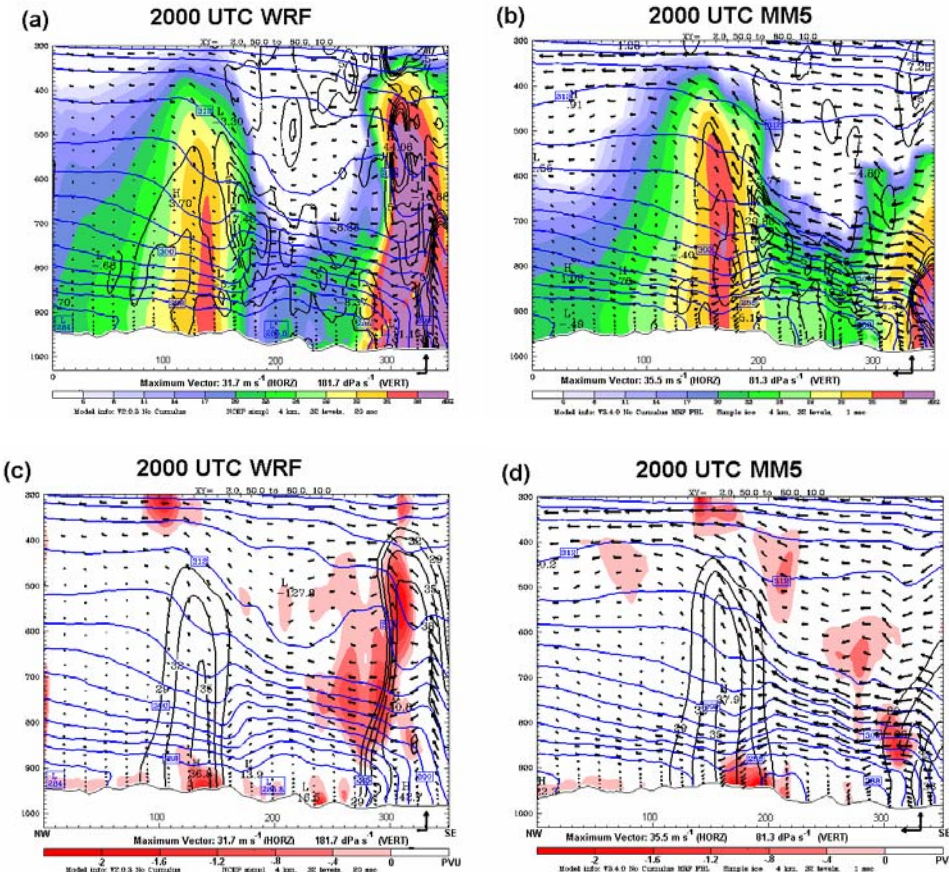


Fig. 6. (a) 4-km WRF 20-h forecast cross section taken through the midlevel frontogenesis maximum (orientation given in Fig. 5a) showing model-simulated reflectivity (shaded according to scale starting at 5 dBZ), Miller 2D frontogenesis [thin solid, positive values contoured every 4°C (100 km) $^{-1} \text{ h}^{-1}$ starting at 1°C (100 km) $^{-1} \text{ h}^{-1}$], saturation equivalent potential temperature (blue solid, contoured every 3 K), and circulation in the plane of the cross section (arrows). (b) Same as in (a), except for the 4-km MM5 20-h forecast (cross-section orientation given in Fig. 5b). (c) Same as in (a), except simulated reflectivity (contoured every 3 dBZ starting at 29 dBZ), and saturation equivalent potential vorticity (shaded where negative according to scale starting at 0 PVU), (frontogenesis not shown). (d) As in (c), except for the MM5 model forecast.

4.2 Microphysical considerations

Although one might expect the forecast band (as defined by the surface simulated reflectivity maximum) to be directly beneath the ascent maximum, both the MM5 and WRF simulations forecast the band 20–40 km farther northwest. In light of the strong east winds evident in the model simulations, it may be hypothesized westward precipitation drift occurred. Evidence for this hypothesis is given by radar cross sections through the band from the Albany, New York, WSR-88D radar (Fig. 7a). A cross section through the band at 2200 UTC 25 December 2002 shows that the 28 dBZ core of the band tilts toward the southeast with height ~ 20 km, suggesting northwestward hydrometeor drift. Also, in the upper levels (~ 500 -hPa) of the model cross sections (Figs. 6a,b) it is noted that the maximum reflectivity was forecast to be just northwest of the ascent maximum. This displacement may be evidence of the time it takes for precipitation production and fallout to occur within the strong slantwise frontal ascent, which is partially dependent on the microphysical scheme used.

4.3 0000 UTC 25 December 2002 ensemble

To further explore the predictability of the 25 December 2002 case, a limited ensemble of simulations using different

initial conditions, convective parameterizations, and boundary layer and microphysics schemes were run using the MM5 and WRF modeling frameworks. Table 1 summarizes characteristics of members composing this ensemble, including whether a member explicitly forecast a band. It is noted that all model simulations had an elongated area of heavy precipitation over eastern New York, but through subjective assessment of the scale, duration, and intensity of this area it was determined that five of the seven members explicitly predicted band formation, suggesting high predictability of the occurrence of band formation in this case. The timing, location, and intensity of the simulated bands varied (not shown) among the five members that explicitly forecast band formation. The two members that did not exhibit band formation (1 and 2) differed from the simulations evaluated in section 4.1 in their use of the Gayno–Seaman (GS; Gayno et al. 1994) boundary layer and Reisner 2 (Thompson et al. 2004) microphysics schemes. This result suggests some sensitivity to the choice of boundary layer and microphysics schemes, which will be explored in future research. Also, given that initial condition uncertainty generally dominates physics uncertainty in cold-season weather regimes in the northeast U.S. (Jones et al. 2005), more diverse initial conditions may provide a better measure of predictability in this case.

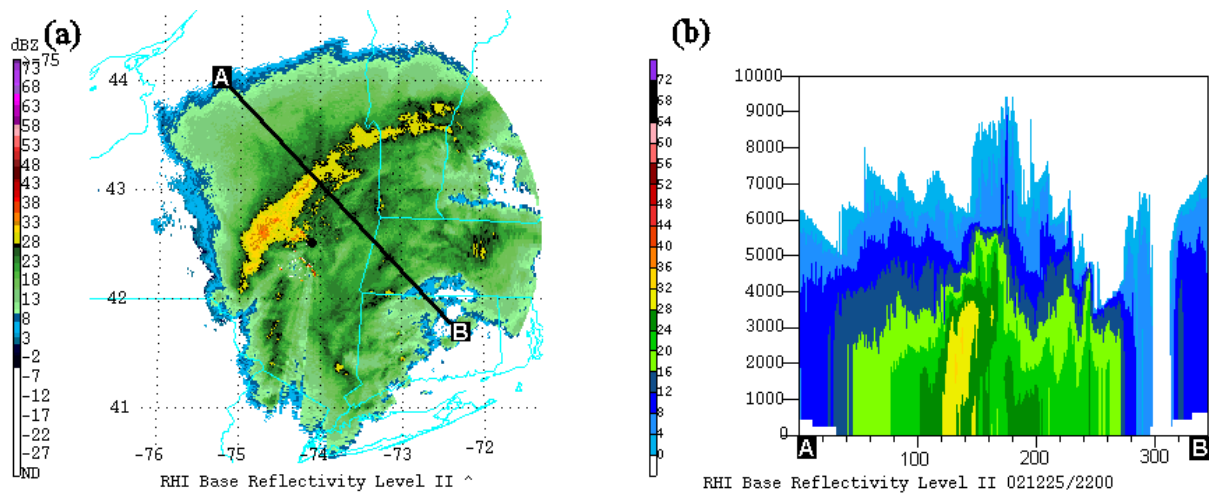


Fig. 7. (a) 2200 UTC 25 December 2002 WSR-88D radar reflectivity (shaded according to scale, dBZ) from the Albany, New York (ENX) WSR-88D radar (radar location marked by black dot). (b) Same as in (a), except for radar reflectivity cross section [orientation shown in (a)].

Table 1: Ensemble member characteristics.

	Model	Initialization	Convection	Boundary Layer	Microphysics	Band?
Member 1	PSU/NCAR MM5	EDAS	Grell	GS	Simple Ice	No
Member 2	PSU/NCAR MM5	EDAS	Grell	MRF	Reisner 2	No
Member 3	PSU/NCAR MM5	GDAS	Grell	MRF	Simple Ice	Yes
Member 4	PSU/NCAR MM5	EDAS	Kain–Fritch	MRF	Simple Ice	Yes
Member 5	NCAR WRF	EDAS	Kain–Fritch	YSU	Lin	Yes
Member 6	NCAR WRF	EDAS	Kain–Fritch	YSU	WSM-3 class	Yes
Member 7	NCAR WRF	EDAS	Grell–Devenyi	MRF	WSM-5 class	Yes

5. SUMMARY

This case study shows that high-resolution versions of the MM5 and WRF models are capable of simulating the primary processes responsible for mesoscale bands. Although the WRF model had a more accurate forecast of the cyclone intensification and precipitation amounts compared to the MM5, the location of initial band formation in the WRF forecast was well south of the observed location. Furthermore, the WRF exhibited the formation of a second band, which was not observed. Conversely, although the MM5 underpredicted the cyclone intensification and precipitation amounts, the location of initial band formation was near the observed location. Both models dissipated the initial band too quickly. Despite these timing and location errors, model forecasts showed a narrow sloping ascent maximum approaching 1 m s^{-1} in the vicinity of the band, associated with strong midlevel frontogenesis and weak moist symmetric stability. A limited ensemble suggested high predictability in the occurrence of band formation, although the timing, location, and intensity of the simulated bands varied. Further research is planned to explore the timing and intensity errors noted in the model simulations, the microphysical aspects of the observed and simulated bands, and the general predictability of the 25 December 2002 event.

6. ACKNOWLEDGMENTS

Yanluan Lin (Stony Brook University) aided in running the ensemble member simulations used in this study. This study was supported in part by UCAR/COMET Grant S02-38662 and NOAA Grant NA04NWS4680005.

7. REFERENCES

Dudhia, J., 1989: Numerical study of convection observed during the winter monsoon experiment using a mesoscale two-dimensional model. *J. Atmos. Sci.*, **46**, 3077–3107.

Gayno, G. A., N. L. Seaman, A. M. Lario, and D. R. Stauffer, 1994: Forecasting visibility using a 1.5-order closure boundary layer scheme in a 12 km non-hydrostatic model. *Preprints, 10th Conference on Numerical Weather Prediction*, Portland, OR, Amer. Meteor. Soc., 18–20.

Grell, G. A., 1993: Prognostic evaluation of assumptions used by cumulus parameterizations. *Mon. Wea. Rev.*, **121**, 764–787.

Han, M., M. K. Ramamurthy, R. M. Rauber, B. F. Jewett, and J. A. Grim, 2003: A modeling study of the frontal circulations associated with a heavy snowband in an extratropical cyclone. *Preprints, 10th Conference on Mesoscale Processes*, Portland, OR, Amer. Meteor. Soc., CD-ROM, 1.11.

Hong, S.-Y., and H.-L. Pan, 1996: Nonlocal boundary layer vertical diffusion in a medium-range forecast model. *Mon. Wea. Rev.*, **124**, 2322–2339.

—, J. Dudhia, and S.-H. Chen, 2004: A revised approach to ice microphysical processes for the bulk parameterization of clouds and precipitation. *Mon. Wea. Rev.*, **132**, 103–120.

Jones, M. S., B. A. Colle, and J. S. Tongue, 2005: Evaluation of a mesoscale short-range ensemble system over the northeast United States. *Wea. Forecasting*. Submitted.

Moore, J. T., C. E. Graves, S. Ng, and J. L. Smith, 2005: A process-oriented methodology toward understanding the organization of an extensive mesoscale snowband: A diagnostic case study of 4–5 December 1999. *Wea. Forecasting*, **20**, 35–50.

Nicosia, D. J., and R. H. Grumm, 1999: Mesoscale band formation in three major northeastern United States snowstorms. *Wea. Forecasting*, **14**, 346–368.

Novak, D. R., L. F. Bosart, D. Keyser, and J. S. Waldstreicher, 2004a: An observational study of cold season–banded precipitation in northeast U.S. cyclones. *Wea. Forecasting*, **19**, 993–1010.

—, J. S. Waldstreicher, L. F. Bosart, and D. Keyser, 2004b: A forecast strategy for anticipating mesoscale band formation within developing extratropical cyclones. *Preprints, 20th Conference on Weather Analysis and Forecasting*, Seattle, WA, Amer. Meteor. Soc., CD-ROM, 8.1.

Sanders, F., and L. F. Bosart, 1985: Mesoscale structure in the megalopolitan snowstorm of 11–12 February 1983. Part I: Frontogenetical forcing and symmetric instability. *J. Atmos. Sci.*, **42**, 1050–1061.

Stoelinga, M. T., 2005: Simulated equivalent reflectivity factor as currently formulated in RIP: Description and possible improvements. Available at: http://www.atmos.washington.edu/~stoeling/RIP_sim_ref.pdf

Thompson, G., R. M. Rasmussen, and K. Manning, 2004: Explicit forecasts of winter precipitation using an improved bulk microphysics scheme. Part I: Description and sensitivity analysis. *Mon. Wea. Rev.*, **132**, 519–542.

Thorpe, A. J., and K. A. Emanuel, 1985: Frontogenesis in the presence of small stability to slantwise convection. *J. Atmos. Sci.*, **42**, 1809–1824.